

# THE USE OF CYCLIC $\Delta J$ AS A PARAMETER FOR FATIGUE INITIATION OF X52 STEEL

J. Capelle<sup>1</sup>, J. Predan<sup>2</sup>, N. Gubeljak<sup>2</sup> and G. Pluinage<sup>3</sup>

<sup>1</sup> LaBPS - Ecole Nationale d'Ingenieurs de Metz  
1 route d'Ars Laquenexy, 57078 Metz, (France)

<sup>2</sup> University of Maribor (Slovenia)

<sup>3</sup> Université de Lorraine 57045, Metz (France)  
Corresponding author pluinage@cegetel.net

**Key Words:** Fatigue initiation,  $\Delta J$  cyclic, acoustic emission, hydrogen absorption.

## Abstract

The concept of  $\Delta J$  cyclic has been extended to fatigue initiation emanating from notch. The parameter is then named  $\Delta J_p$ . Validation of this parameter is made by fatigue tests made on Roman tile specimens made in X52 pipe steel. Here, fatigue initiation is detected by acoustic emission. It has been found that the fatigue initiation decreases after hydrogen absorption. This can be explained by interaction of hydrogen and plasticity as can be seen for tensile and fracture behaviour of X52 steel after introduction of hydrogen.

## Introduction

The number of cycles to fatigue failure  $N_f$  is the sum of the number of cycles to initiation  $N_i$  and the number of cycles of crack propagation  $N_p$ . The ratio of the number of cycles to initiation and the number of cycles to failure is not constant. It increases when the number of cycles increases: for low cycle fatigue, this ratio is about 0.6 and for high cycle fatigue it is more than 0.9 and reaches the unit value at endurance limit. For this reason, for high cycle fatigue the following approximation is generally used  $N_i \approx N_f$ .

Crack propagation is easily detected by microscope observation but the early start of propagation is difficult to detect and is generally done by tools like acoustic emission and infrared thermography [1]. Detection of early stage of crack propagation suffers on the fact that due to constrain, crack initiates first at mid thickness than before on surface. This leads on a non-conservative value of number of cycles to initiation. Acoustic emission is emitted with burst energy overcoming a conventional threshold. Sufficient slip bands on metal surface are then activated and allowed intrusions and extrusions able to promote crack starting. This technique gives a conservative value of  $N_i$ . Infrared red thermography detects increasing temperature due to plastic dissipation at crack tip. The use of this non conservative method is very seldom and allows to detect crack initiation with a high sensibility. All these technical difficulties explain that majority of paper in literature presents fatigue results where number of cycles to initiation is approximated to number of cycles to failure. Fatigue resistance to initiation is then represented by a power relationship of types  $P_i = f(N_i^b)$  where  $P_i$  is an initiation parameter and  $b$  exponent of Basquin's type. Several approaches have been used to define the initiation parameter  $P_i$ : effective stress, notch stress intensity factor or damage parameter issued from Smith-Watson and Topper (SWT) parameter [2].

In this paper we have extend the concept of  $\Delta J$  cyclic to fatigue initiation emanating from notch. The parameter is then named  $\Delta J_p$ .

Validation of this parameter is made by fatigue tests performed on Roman tile specimens made in X52 pipe steel. Here, fatigue initiation is detected by acoustic emission.

Results obtained on the same material after hydrogen absorption are analysed in order to extend the validity of the fatigue initiation criterion whatever the large scatter obtained in number of cycles to initiation after introduction of hydrogen.

## Material

The objects of study is the API 5L X52 grade pipeline steel. The chemical composition of this steel is given in Table 1.

Table 1: Chemical composition of steel API 5L X52

C	Mn	Si	Cr	Ni	Mo	S	Cu	Ti	Nb	Al
0.206	1.257	0.293	0.014	0.017	0.006	0.009	0.011	0.001	<0.03	0.034

Table 2: Tensile properties of X52 steel in air and with hydrogen absorption

	$\sigma_y$ (MPa)	$\sigma_{ul}$ (MPa)	A%
Air	410	528	15.8
Hydrogen	420	570	9.76

Stress strain curves of X52 steel have been determined with and without hydrogen absorption and reported in figure 1. Classical tensile properties such as yield stress and ultimate strength increases also when hydrogen is absorbed in steel as indicated in Table 2. A small increase of yield stress has been noted (2,5%) and an important reduction of elongation at failure (38%) .

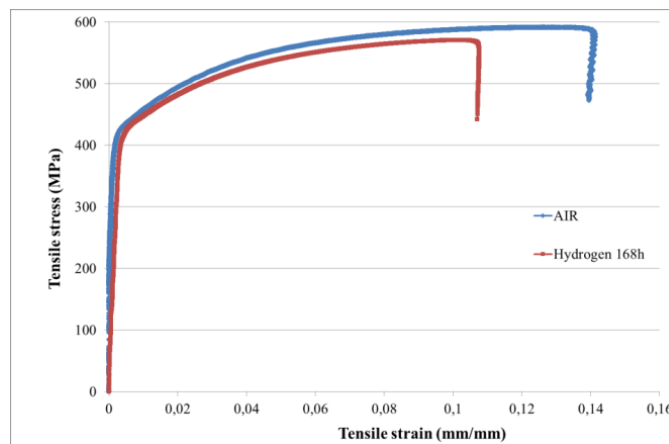


Figure1: stress strain curves of X52 pipe steel with and without hydrogen absorption

Static stress-strain is obtained by fitted tensile test results using hardening power law:

$$\sigma = K \varepsilon^n \quad (1)$$

The cyclic strain energy density is defined as the area under the ascending branch of the fatigue hysteresis loop. This branch is described by the following power law:

$$\sigma = K'' \varepsilon^{n''} \quad (2)$$

where  $K^*$  is a coefficient and  $n''$  the hysteresis loop strain hardening exponent.

The different parameters of static and cyclic stress-strain behaviours are given in table 3. The cyclic  $\Delta J$  integral will be computed with parameters of equation (2) because no major difference was detected with and without hydrogen introduction.

Table 3: Parameters of static and cyclic stress-strain behaviour

Equation		
(1)	$K = 773 \text{ MPa}$	$n = 0.105$
(2)	$K'' = 755 \text{ MPa}$	$n'' = 0.32$

## Test methods

The fatigue resistance to initiation of the API 5L X52 steel has been measured in radial direction at room temperature using non-standard curved notched specimens, namely, “Roman tile”[3] specimens because the pipe dimensions do not permit to measure through thickness mechanical characteristics. The specimen shape is a circle arc, corresponding to central angle of  $160^\circ$  of 60 mm length. The specimen thickness is 6.1mm. The V-notch with the notch opening angle of  $45^\circ$  and root radius of 0.15 mm was machined to a depth of size  $a$  with the initial notch aspect ratio  $a/W = 0.5$ .

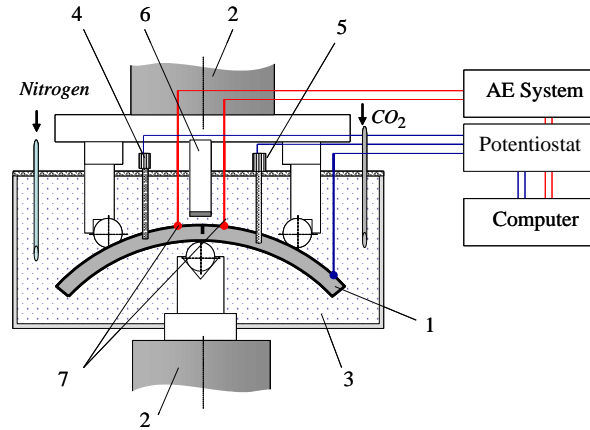


Figure 2 : Roman Tile specimen fixture and assembly Positions of electrodes for hydrogen charging. 1 – Roman tile specimen; 2 – Actuator; 3 – corrosion cell with NS4 solution; 4 – pH electrode; 5 – Reference electrode; 6 – Platinum auxiliary electrode; 7 – AE sensors.

The test set-up of three-point bend test for “roman tile” specimens and testing machine with the bend-test fixture are similar than these used for static test and are described in figure 2. The bend-test fixture was positioned on the closed loop hydraulic testing machine with a load cell of capacity 10 kN. The applied load, frequency and the fatigue cycle (sinusoidal) were monitored on the control panel. Hydrogen charging was made using the same cell filled with NS4 solution. Tests conditions are given in Table 4.

Table 4: Fatigue test conditions

Shape of the cycle used	Sinus:
Frequency :	0.05 Hz
Load ratio	0.5
Working potential	- 1 V <sub>sce</sub>
Electrolytic solution	New Solution 4 (NS4)
Solution pH	between 6.66 and 6.74

Acoustic emission (AE) is registered during test by two sensors as can be seen in position 7 in Figure 2. Fatigue initiation is easily detected by the first important energy.

## Hydrogen charging method

Specimens are hydrogen charged in NS4 solution [3] at some constant potential of polarisation, which is slightly negative than free corrosion potential for the given steels. The hydrogen-charging process is controlled by registration of the cathodic polarisation current  $I_{cath}(\tau)$ . The total quantity of evaluated hydrogen on metal surface can be assessed as ( $E_{cath}$  the cathodic potential)

$$Q_H^{ev} = \int_0^{\tau_{exp}} I_{cath}(\tau) d\tau \quad \text{under } E_{cath} = \text{const.} \quad (3)$$

## Experimental results

The classical power fit of the stress range versus the number of cycles to failure is in accordance with Basquin's law:

$$\Delta\sigma = \sigma'_f (NR)^b \quad (4)$$

where  $\sigma'_f$  is the fatigue resistance and  $b$  the Basquin's exponent. Results are presented in Table 5.

Stress range versus number of cycles to initiation is fitted in Figure 5 by a power law similar to Basquin's one.

$$\Delta\sigma = \sigma'_i (N_i)^\beta \quad (5)$$

Table 5: Fatigue resistance parameters with and without hydrogen charging for X 52 steel.

	Air	H <sub>2</sub>
	At failure	At failure
Fatigue resistance $\sigma'_f$	339 MPa	301 MPa
Basquin's exponent $b$	- 0.0202	-0.012

where  $\sigma'_i$  is fatigue initiation resistance and  $\beta$  an exponent.  $\Delta\sigma$  is the gross stress range.

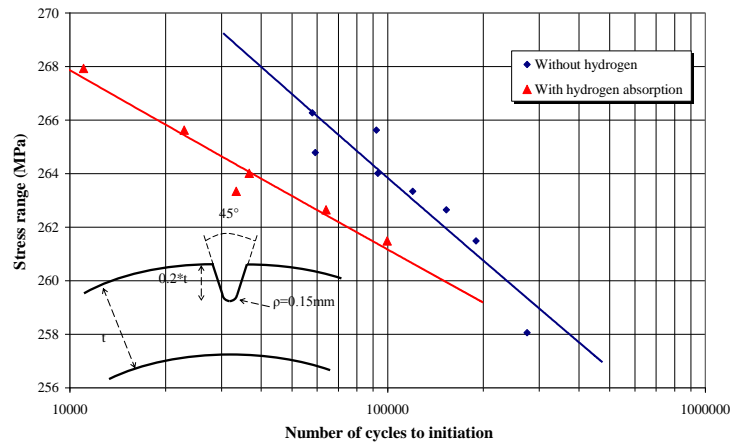


Figure 3 : Fatigue initiation resistance curves for Steel API 5L X52 with and without hydrogen absorption.

Table 6: fatigue initiation resistance and  $\beta$  exponent for steel API 5L X52

	Fatigue initiation resistance $\sigma'_i$ (MPa)	Exponent $\beta$	$R^2$
Without	320	-0.0220	0.8843
With hydrogen	296	-0.011	0.9502

## Determination of $\Delta J_\rho$

Following the original definition of J-integral for monotonic loading for Cartesian coordinates with the  $x$  axis parallel to the crack face and any crack tip encircling contour  $\Gamma$  beginning from the bottom surface of the crack and ending at the top surface, the cyclic J-integral is defined by :

$$\Delta J_{cycl} = \int_{\Gamma} W^*_{cycl} dy - T_{ij} \frac{\partial u_i}{\partial x} ds \quad (6)$$

here  $W^*_{cycl}$  is the cyclic strain energy density defined by the following relationship:

$$W_{cycl}^* (\Delta \varepsilon_{mn}) = \int_0^{\Delta \varepsilon_{mn}} \Delta \sigma_{ij} d\varepsilon_{kl} = \int_0^{\varepsilon_{mn}^{(j)} - \varepsilon_{mn}^{(i)}} [\sigma(j)_{kl} - \sigma(i)_{kl}] d\varepsilon_{kl} \quad (7)$$

$T_{ij}$  are the surfacic tensions and  $u_i$  displacement. It has been proof that this integral is also path independent [4].  $\Delta J_p$  is computed according to equation (7) with the cyclic stress strain curve given by equation (2). The maximum load used in computing is equal to load range and minimum load correspond to load origin.

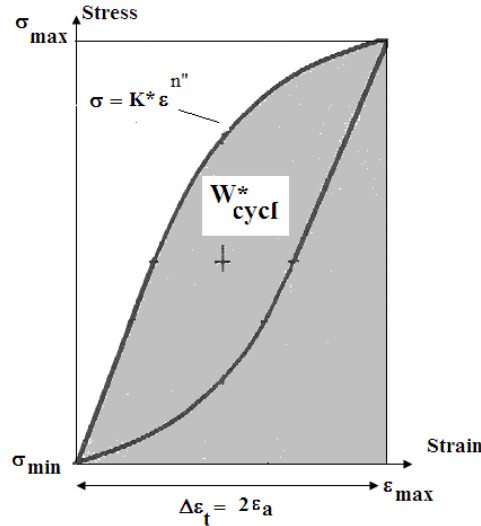


Figure 4: Definition of the cyclic strain energy density. Note that the origin is defined at the lower part of the hysteresis loop.

The numerical analyses were done for a simplified two-dimensional FE model of the “Roman Tile” specimen. Since the specimen is symmetric with respect to the crack plane, only the half of the specimen is modeled. No real crack extension during cyclic loading is modeled. Instead, we assume a specimen with a notch radius 0.25 mm subjected to mechanical loading between minimum and maximum load,  $F_{min}$  and  $F_{max}$ . For the given values of applied load  $F_{max}$ , the load ratio is equal to  $R=0.5$ .

The analyses are performed using a commercial implementation of the finite element method (ABAQUS, [http://www.simulia.com/products/abaqus\\_fea.html](http://www.simulia.com/products/abaqus_fea.html)). Hereby small strain formulations are adopted. Two-dimensional 8-node elements are used, as they give much better results than the first order elements. In order to get sufficient accuracy, the mesh sizes at the notch must be sufficiently small. The smallest mesh size is 0.0016 mm around the notch region. The elastic-plastic material behavior is modeled using the incremental plasticity model provided by ABAQUS. For strains smaller than the yield strain, the material is modeled as linear elastic. For strains larger than the yield strain, hardening according to the cyclic stress strain curves is adopted.

Thus, deformation theory of plasticity is used in the post-processing procedure, i.e. the material is treated as if it were non-linear elastic. Such a treatment is conventionally used when applying the  $J$ -integral concept to elastic-plastic. The equilibrium stress and strain fields are computed for mechanical loading. The effect of hydrogen embrittlement is introduced by using stress strain curves obtained after hydrogen introduction.

The notch cyclic  $J$ -integral range  $\Delta J_p$  values are calculated using the virtual crack extension method of ABAQUS [5]. A rectangular contour including all notch radius elements is used for the evaluation of the  $J$ -integral. A calibration curve  $\Delta J_p$  versus the maximum load is obtained and used for drawing resistance to fatigue initiation curve as  $\Delta J_p$  versus number of cycles to initiation (figure 5).

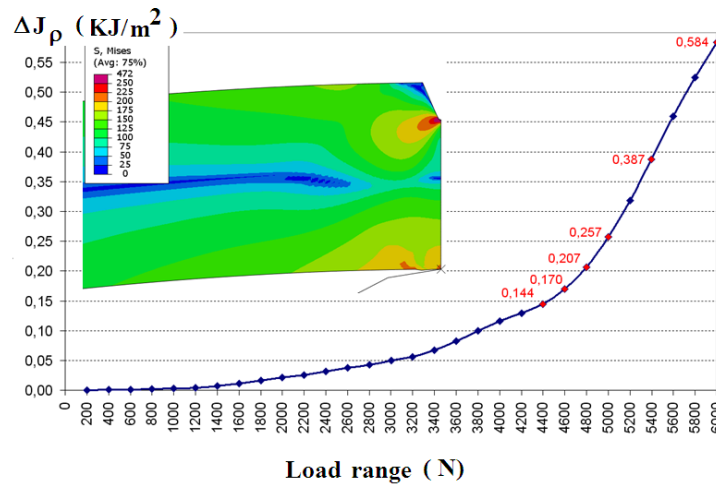


Figure 5 : calibration curve  $\Delta J_p$  versus the maximum load.  
(In red the corresponding  $\Delta J_p$  values in KJ/m<sup>2</sup> to the load range listed in Table 7).

Resistance to fatigue initiation curves as  $\Delta J_p$  versus number of cycles to initiation with and without hydrogen introduction are plotted and reported in figure 6, data are given in table 7.

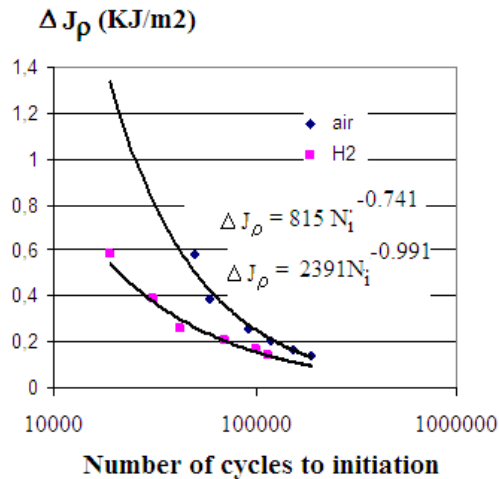


Figure 6 : Fatigue initiation curve  $\Delta J_p = f(N_i)$  for X52 steel.

### Influence of hydrogen on mechanical properties of x52 steel

In order to analyse the influence of hydrogenating environments on mechanical behaviour of ferritic steels, many factors should be taken into account: environmental, surface and metallurgical conditions and hydrogen physical behaviour are the main factors that influence the complex problem of hydrogen embrittlement. Hydrogen embrittlement micromechanisms are hydrogen solubility, diffusivity and trapping which depend on the steel microstructure, temperature, stresses state and, finally, on the presence of lattice defects as vacancies, alloying elements, dislocations interfaces, microvoids and grain boundaries.

Many embrittlement models are available, but no one is applicable to all the possible conditions. Among them, one notes:

- Models based on the internal pressure, due to molecular recombination in microvoids or at interfaces with crack initiation and growing under high hydrogen pressure.
- Lynch [6] proposed an interatomic bonds weakening by hydrogen adsorption at the crack tip. Localized plastic straining would then lead to the formation of microvoids ahead of the crack tip. Crack propagation would then occur by microvoid coalescence.

- Troiano [7] and further developed by Oriani [8]. Hydrogen insertion in solid solution would decrease the forces required to fracture the metal along the crystal lattice i.e. decrease cohesion forces of the lattice and the energy necessary to induce cleavage,
- Other models are based on hydrogen induced local plasticity. Beachem [9] proposed that hydrogen absorbed at crack tip enhances dislocations glide and therefore plastic strain processes leading to metal fracture. In the hydrogen enhanced localized plasticity (HELP) model, hydrogen increases dislocations mobility. Dislocations can then pile-up more easily, resulting in a distribution of microscopic highly strayed areas surrounded by less ductile areas.
- Models based on the hydrides precipitation or fragile phases formation (e.g. formation of  $\alpha'$ , cc, or  $\epsilon$ , hc, martensitic phases in metastable austenitic stainless steels that could be hydrogen induced).

In order to check the possible hydrogen embrittlement mechanisms for low strength ferritic steel, we have examined the influence of hydrogen absorption on stress strain curve and on fracture energy.

Examination of evolution of tensile and fracture properties of X52 pipe steel (see figure 7) lead to the assumption that fatigue initiation under hydrogen is promoted by interaction of hydrogen and plastic deformation coupled with reduction of cohesive energy. With hydrogen absorption, API 5L X52 remains ductile whatever a strong reduction in elongation to fracture and fatigue initiation occurs by formation of dislocation cells and slipping bands. The mechanism is controlled by plastic shearing strain. When hydrogen is absorbed in metals, hydrogen atoms pin dislocations. A necessary increase in shearing stress is needed to move dislocation.

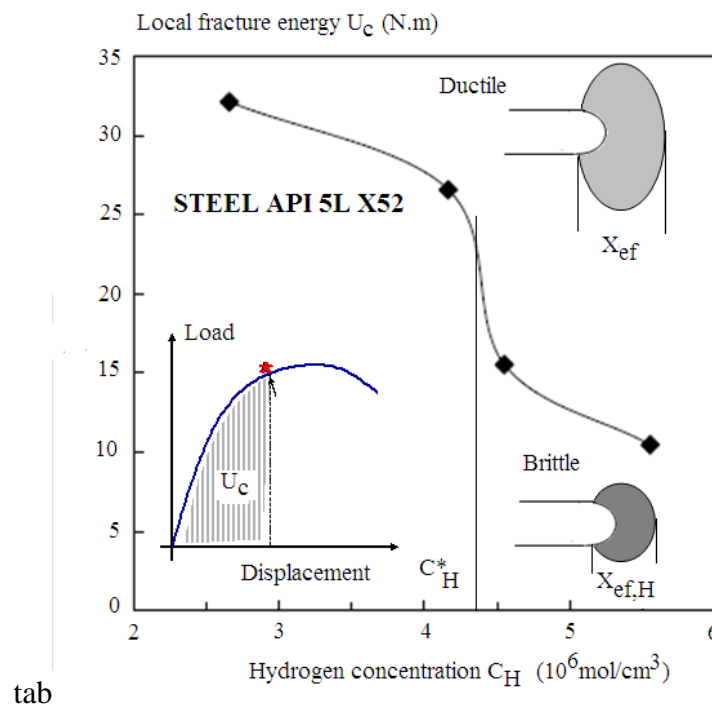


Figure 7: Ductile-brittle transition with hydrogen concentration in API5L X52 steel.

The new facts introduced by this study are:

Fatigue initiation appears in X52 pipe steel earlier with hydrogen absorption and the ratio number of cycles to initiation to life duration is higher than without hydrogen absorption. This means that the effect of hydrogen is more pronounced in fatigue crack propagation than in fatigue initiation. Fatigue initiation is sensitive to hydrogen enhanced localized plasticity (HELP) but fatigue crack propagation is sensitive to HELP and reduction of cohesive energy.

Scatter in number of cycles to initiation with hydrogen absorption is strongly increased probably by enhanced localized plasticity produces by surface dislocations.

## Conclusion

The cyclic  $\Delta J_p$  integral is used as a fatigue initiation parameter and derives from the  $\Delta J$  parameter introduced by several authors [10],[11]. This parameter is computed by finite element method from the cyclic stress-strain behaviour obtained from the hysteresis loop and takes into account the notch radius of the specimen. This parameter is similar to other fatigue initiation parameter like effective stress at notch tip. It is a little faster to obtain and can be considered as a function of cyclic strain energy dissipated at notch tip. It doesn't need any assumption on fatigue process volume. This fatigue initiation parameter has been used to compare the fatigue resistance of X52 pipe steel before and after hydrogen absorption. It has been found that fatigue initiation decreases with hydrogen absorption. This important lost of fatigue resistance can be explained by interaction of hydrogen and plasticity as can be seen for tensile and fracture behaviour of X52 steel after hydrogen introduction.

## REFERENCES

- [1] T.Ummenhofer J.Medgenberg. On the use of infrared thermography for the analysis of fatigue damage processes in welded joints. *International Journal of Fatigue*, Vol 31, Issue1, January, (2009).
- [2] K. N.Smith, P.Watson, and T. H. Topper, A stress-strain function for the fatigue of metals. *Journal of Materials, JMLSA*, 5, 767-778, (1970).
- [3] J. Capelle, J. Gilgert, I. Dmytrakh, G. Pluvinage, The effect of hydrogen concentration on fracture of pipeline steels in presence of a notch, *Engineering Fracture Mechanics*, Volume 78, Issue 2, January, pp 364-373,(2011).
- [4]C.L. Chow and T.J. Lu. Cyclic  $J$ -integral in relation to fatigue crack initiation and propagation *Engineering Fracture Mechanics*, Vol 39,Issue 1, pp 1-20, (1991).
- [5] [www.simulia.com](http://www.simulia.com) (Abaqus)
- [6] S.P. Lynch., *Acta Metallurgica*, v36, 2639, (1988).
- [7] A.Troiano, Transactions of ASM, v52, 54, (1960).
- [8] R. Oriani,In. R.Staehle, J.Hochmann, R.McCright Eds, Stress corrosion cracking and hydrogen embrittlement of iron base alloy. Houston: *NACE*, 351,(1977).
- [9] C.D. Beachem, *Metallurgical Transactions*, v3, 437, (1972).
- [10] K.Tanaka, The cyclic  $J$ -integral as a criterion for fatigue crack growth, *Int. J. Fracture*, Vol. 22, 1983, pp. 91-104;
- [11] D.Rozumek:  $J$ -integral in the description of elastic-plastic crack growth kinetics curve, *The Archive of Mechanical Engineering*, Vol. LIII, No. 3, 2006, pp. 211-225.